NASA TECHNICAL NOTE

NASA TN D-5855

c. 1

TECH LIBRARY KAFB, NM

0132575

NASA TN D-5855

EFFECT OF BLADE LEADING EDGE THICKNESS ON CAVITATION PERFORMANCE OF 80.6° HELICAL INDUCER IN HYDROGEN

by Royce D. Moore and Phillip R. Meng

Lewis Research Center
Cleveland, Ohio 44135

NATIONAL AERONAUTICS AND SPACE ADMINISTRATION • WASHINGTON, D. C. • JUNE 1970

TECH LIBRARY KAFB, NM

0132575

1. Report No. NASA TN D-5855	2. Government Accession No.	3. Recipient's Catalog No.
4. Title and Subtitle EFFECT OF BLADE LEADING EDGE THICKNESS ON CAVITATION PERFORMANCE OF 80.6° HELICAL INDUCER IN HYDROGEN		5. Report Date June 1970
		6. Performing Organization Code
7. Author(s) Royce D. Moore and Phillip R. Meng		8. Performing Organization Report No. E-5445
9. Performing Organization Name and Address Lewis Research Center National Aeronautics and Space Administration Cleveland, Ohio 44135		10. Work Unit No. 128-31
		11. Contract or Grant No.
		13. Type of Report and Period Covered Technical Note
12. Sponsoring Agency Name and Address National Aeronautics and Space Administration Washington, D.C. 20546		14. Sponsoring Agency Code

15. Supplementary Notes

16. Abstract

Three different 80.6° helical inducers were tested in hydrogen over a range of liquid temperatures and flow coefficients. These inducers were identical in design except for the blade leading edge thickness. Although no consistent trend was observed with thickness, the required net positive suction head NPSH for each thickness increased with increasing flow coefficient and decreased with increasing liquid temperature. The predicted thermodynamic effects of cavitation varied with blade leading edge thickness. Two cavitation parameters that qualitatively evaluate the cavitation performance of inducers were developed.

17. Key Words *(Suggested by Author(s))* Cavitation Liquid hydrogen Inducers	18. Distribution Statement Unclassified - unlimited

19. Security Classif. (of this report)	20. Security Classif. (of this page)	21. No. of Pages	22. Price*
Unclassified	Unclassified	22	$3.00

*For sale by the Clearinghouse for Federal Scientific and Technical Information Springfield, Virginia 22151

EFFECT OF BLADE LEADING EDGE THICKNESS ON CAVITATION PERFORMANCE OF 80.6° HELICAL INDUCER IN HYDROGEN

by Royce D. Moore and Phillip R. Meng

Lewis Research Center

SUMMARY

Three different 80.6° helical inducers were tested in liquid hydrogen at a rotative speed of 30 000 rpm. These inducers were identical in design except for the blade leading edge thickness. The experimental inducers were tested over a liquid temperature range of 31.0° to 39.2° R (17.2 to 21.8 K) and a flow coefficient range of 0.082 to 0.118. The net positive suction head NPSH requirements for each inducer increased with increasing flow coefficient and decreased with increasing liquid temperature. The NPSH requirements were considerably different for the three blade leading edge thicknesses. However, no consistent trend with blade leading edge thickness was observed. The predicted thermodynamic effects of cavitation were the greatest for the inducer with the thickest blade leading edge and the smallest for the inducer with the medium-thin blade leading edge. Two cavitation parameters that qualitatively evaluate the performance of inducers were developed. The noncavitating head rise was highest over the entire flow range for the inducer with the thinnest blade leading edge and lowest for the inducer with the thickest blade leading edge.

INTRODUCTION

Inducers used in rocket-engine turbopumps are designed to operate satisfactorily with cavitation present on the suction surface of the blades. The required net positive suction head NPSH for an inducer operated at a given cavitating performance level has been shown to vary with the liquid, the liquid temperature, and the rotative speed and flow rate at which the inducer is operated (refs. 1 to 5). This variation in required NPSH has been attributed to the thermodynamic effects of cavitation. Venturi cavitation studies (ref. 6) have shown that the magnitude of these thermodynamic effects also depends on the surface pressure distribution, that is, local liquid velocities and pressures

that influence the heat- and mass-transfer rates.

For inducers, variations in blade leading edge thickness, blade shape, and blade helix angle will affect the pressure distribution on the blade suction surface and, thus, should affect the magnitude of the thermodynamic effects of cavitation. In the present study, only changes in blade leading edge thickness are considered.

In previous investigations (refs. 4 and 5), the cavitation performance of two different 80.6° helical inducers was determined in liquid hydrogen. These two inducers differed only in blade leading edge thickness. For the present investigation, the blade leading edge thickness is between those of the inducers of references 4 and 5.

The objective of this investigation was to determine the effect of blade leading edge thickness on the cavitation performance of an 80.6° helical inducer. The variation of the thermodynamic effects of cavitation with blade leading edge thickness is also investigated. Two cavitation parameters that qualitatively evaluate the performance of the inducer are developed. The experimental inducers were tested in liquid hydrogen at a rotative speed of 30 000 rpm. The liquid temperature ranged from 31.0° to 39.2° R (17.2 to 21.8 K), and the flow coefficients ranged from 0.082 to 0.118. This investigation was conducted at the Plum Brook Station of the NASA Lewis Research Center.

APPARATUS AND PROCEDURE

Test Inducers

The three experimental inducers used in this investigation were identical in design except for the blade leading edge thickness. Each rotor was a three-bladed flat-plate

TABLE I. - GEOMETRIC DETAILS OF 80.6° HELICAL INDUCER

Tip helix angle (from axial direction), deg	80.6
Rotor tip diameter, in. (cm)	4.980 (12.649)
Rotor hub diameter, in. (cm)	2.478 (6.294)
Hub-tip ratio	0.496
Number of blades	3
Axial length, in. (cm)	2.00 (5.08)
Peripheral extent of blades, deg	280
Tip chord length, in. (cm)	12.35 (31.37)
Hub chord length, in. (cm)	6.36 (16.15)
Solidity at tip	2.350
Tip blade thickness, in. (cm)	0.100 (0.254)
Hub blade thickness, in. (cm)	0.150 (0.381)
Calculated radial tip clearance at hydrogen temperature, in. (cm)	0.025 (0.064)
Ratio of tip clearance to blade height	0.020
Material	6061-T6 Aluminum

helical inducer with a tip helix angle of 80.6°. The inducers had a constant tip diameter of 4.980 inches (12.649 cm) and a hub- to tip-diameter ratio of 0.496. The significant geometric features for the three inducers are given in table I. The three inducers are presented in figure 1 and the leading edges of the inducer blades are shown in figure 2. The inducer with the thinnest leading edge blades is referred to as inducer A; the inducer with the medium-thin leading edge blades is inducer B; and the inducer with the thickest leading edge blades is inducer C.

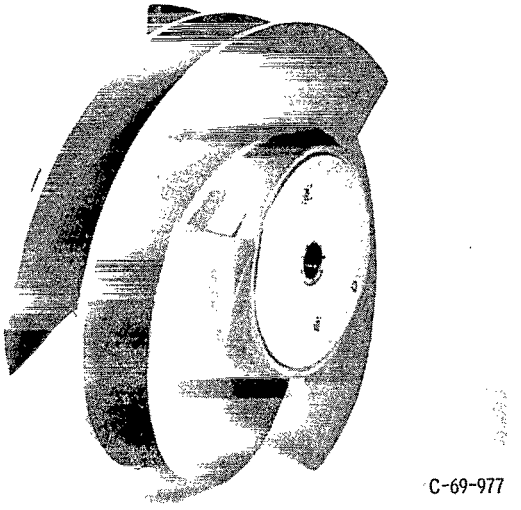

C-69-977

(a) Inducer A.

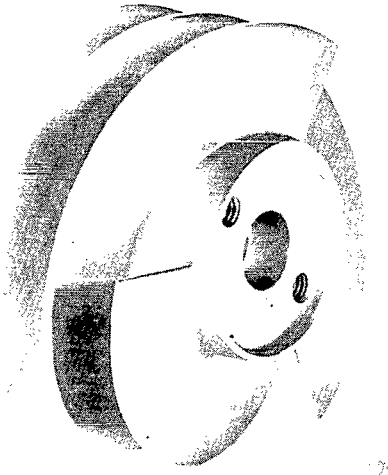

C-69-1669

(b) Inducer B.

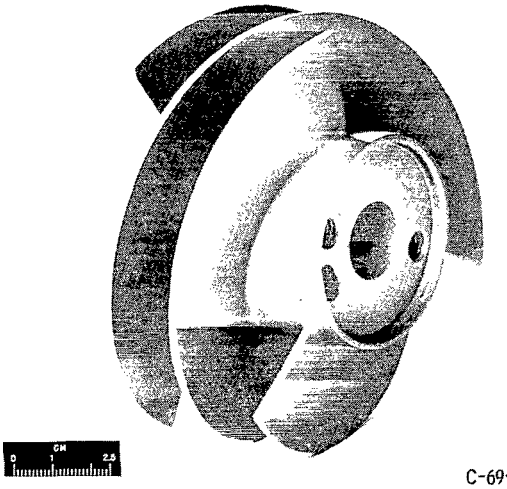

C-69-1670

(c) Inducer C.

Figure 1. - 80.6° Helical inducers.

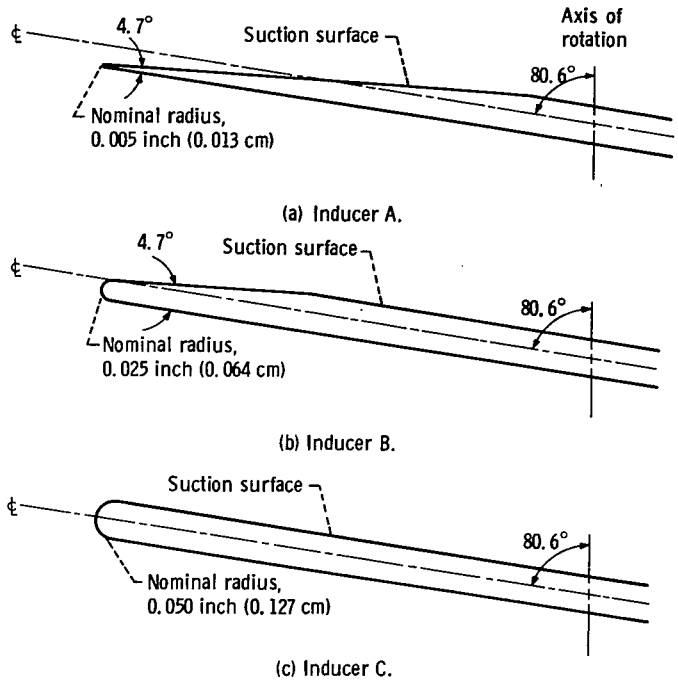

Figure 2. - Blade leading edges for three 80.6° helical inducers.

This investigation was conducted in the liquid hydrogen pump test facility shown schematically in figure 3. The inducer was installed in an inlet annulus that extends 26.5 inches (67.3 cm) above the blade leading edges. The inducer was located near the bottom of the 2500-gallon (9.5-m^3) vacuum-jacketed research tank. A booster rotor

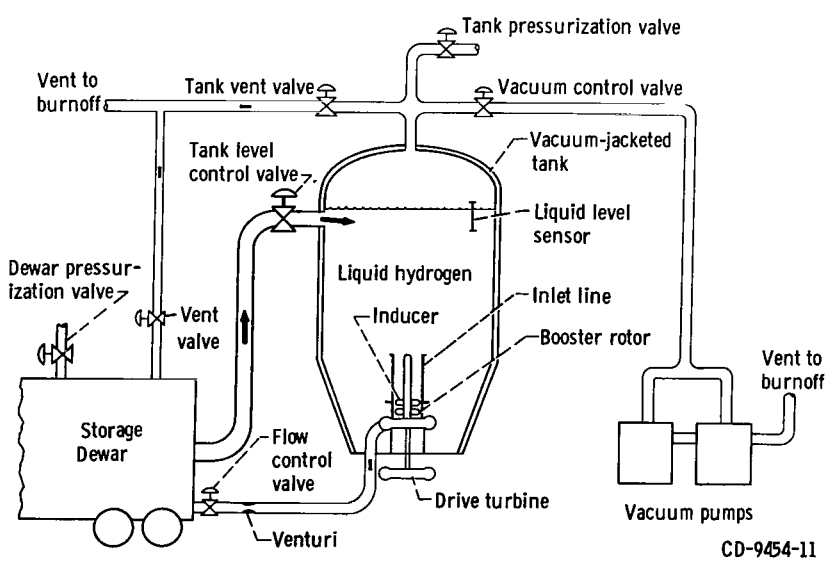

Figure 3. - Liquid hydrogen pump test facility.

located downstream of the inducer was used to overcome system losses. The flow path is down the inlet annulus, through the inducer and booster rotor to a collector scroll, and into a discharge line to the storage Dewar. For test runs above 36.5° R (20.3 K), the liquid was recirculated through the research tank to extend run time.

The facility is basically the same as that described in references 1, 2, and 7.

Test Procedure

The research tank was filled with liquid hydrogen from the storage Dewar. Prior to each test, the hydrogen in the tank was conditioned to the desired liquid temperature by vacuum for runs below 36.5° R (20.3 K) and by recirculation of the liquid for the warmer runs. The tank was then pressurized to 15 psi (10.4 N/cm^2) above the vapor pressure. When the desired rotative speed was attained, the tank pressure (NPSH) was slowly reduced until the head rise deteriorated because of cavitation. The flow rate, rotative speed, and bulk liquid temperature were maintained essentially constant during each test. The noncavitating performance was obtained by varying the flow rate while maintaining a constant rotative speed and liquid temperature. The tank pressure for the noncavitating runs was maintained at 15 psi (10.4 N/cm^2) above the vapor pressure.

The location of the instrumentation used in this investigation is shown schematically in figure 4. The measured parameters and the estimated maximum system errors are also listed in this figure.

The vapor pressures were measured with vapor pressure bulbs that were charged with hydrogen from the tank. One vapor pressure bulb was located at the entrance to the inlet line. The other vapor pressure bulb was located at the inducer inlet. Tank pressure, measured in the ullage space, was used as the reference pressure for the differential pressure transducers. The liquid level above the inducer, measured by a capacitance gage, was added to the reference pressure to correct the differential pressures to the inducer inlet conditions. An averaged hydrogen temperature at the inducer inlet was obtained from two platinum resistor thermometers. A shielded total-pressure probe located at midstream approximately 1 inch (2.54 cm) downstream of the test rotor was used to measure the inducer pressure rise. Pump flow rate was obtained with a Venturi flowmeter that was calibrated in water.

The differential pressure measured directly between tank pressure and the vapor bulb at the annulus inlet was converted to feet of head (m of head) to obtain tank NPSH. Inducer NPSH was obtained by subtracting the inlet-line losses from the tank NPSH. The losses were calculated by multiplying the inlet line fluid velocity head by the loss coefficient of the inlet line, which was determined to be 0.2 from calibrations in air.

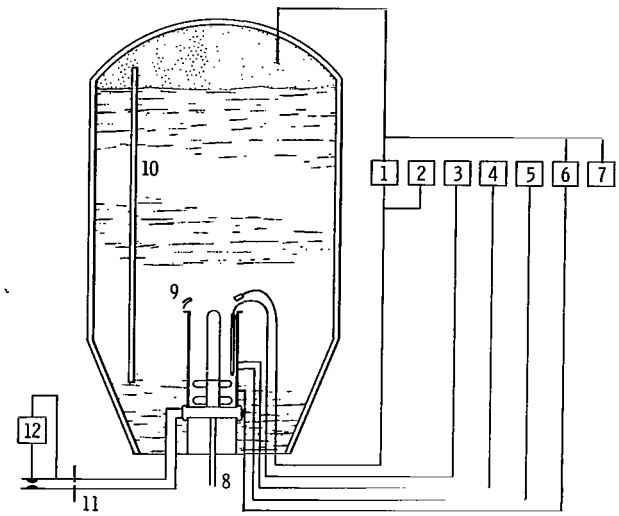

Item number	Parameter	Estimated system accuracy	Number of instruments used	Remarks
1	Tank net positive suction head, psi (N/cm^2)	Low range ±0.05 (±0.035)	1	Measured as differential pressure (converted to head of liquid) between vapor bulb at line inlet and tank pressure corrected to line inlet conditions
		High range ±0.25 (±0.17)	1	
2	Vapor pressure at line inlet, psi (N/cm^2)	±0.25 (±0.17)	1	Vapor bulb charged with liquid hydrogen from research tank
3	Vapor pressure at inducer inlet, psi (N/cm^2)	±0.25 (±0.17)	1	Long, small-diameter vapor bulb with streamlined trailing edge alined with flow stream to minimize bulb cavitation
4	Static pressure (line), psi (N/cm^2)	±0.05 (±0.035)	1	Average of three pressure taps (120° apart) located 10.5 in. (26.6 cm) above inducer inlet
5	Total pressure (line), psi (N/cm^2)	±0.05 (±0.035)	1	Shielded total pressure probe located 0.065 in. (0.165 cm) in from wall and 10.5 in. (26.6 cm) upstream of inducer
6	Inducer pressure rise, psi (N/cm^2)	±1.0 (±0.69)	1	Shielded total pressure probe at mid-passage 1 in. (2.54 cm) downstream of inducer
7	Tank pressure, psi (N/cm^2)	±0.5 (±0.35)	1	Measured in tank ullage and corrected to inducer inlet conditions for reference pressure for differential transducers
8	Rotative speed, rpm	±150	1	Magnetic pickup in conjunction with gear on turbine drive shaft
9	Line inlet temperature, °R (K)	±0.1 (±0.06)	2	Platinum resistor probes 180° apart at inlet
10	Liquid level, ft (m)	±0.5 (±0.15)	1	Capacitance gage, used for hydrostatic head correction to inducer inlet conditions
11	Venturi inlet temperature, °R (K)	±0.1 (±0.06)	1	Platinum resistor probe upstream of Venturi
12	Venturi differential pressure, psi (N/cm^2)	±0.25 (±0.17)	1	Venturi calibrated in air

Figure 4. - Instrumentation for liquid-hydrogen pump test facility.

RESULTS AND DISCUSSION

The noncavitating and cavitating performance of inducers A and C has been reported previously in references 4 and 5, respectively. The thermodynamic effects of cavitation were also evaluated for these two inducers. The performance and evaluation of inducer B are presented first. Then, the performance of the three inducers is compared. Finally, two parameters that qualitatively evaluate the cavitation performance of the three inducers are discussed.

Performance of Inducer B

Noncavitating performance. - The noncavitating performance of inducer B is presented in figure 5. The head-rise coefficient ψ is plotted as a function of flow coefficient φ. Several nominal hydrogen temperatures are shown for a rotative speed of 30 000 rpm. No measurable effect of liquid temperature was noted on the noncavitating head-rise coefficient. The head-rise coefficient decreases almost linearly with increasing flow coefficient over the range studied.

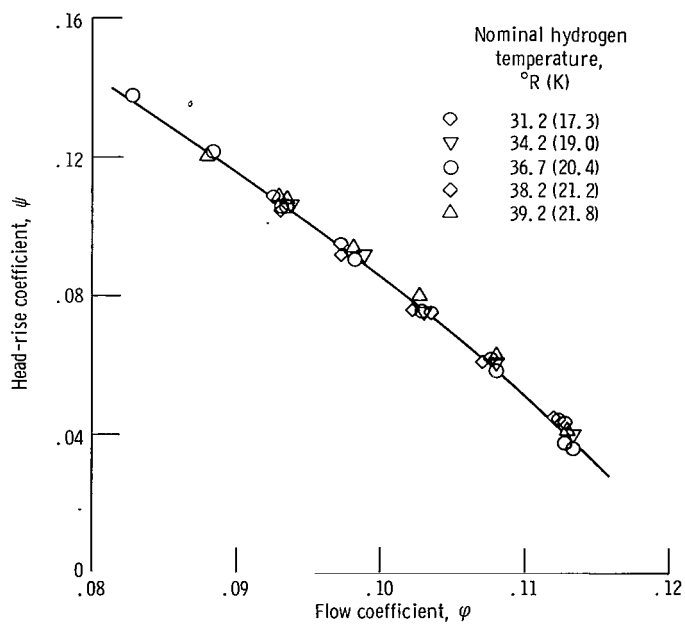

Figure 5. - Noncavitating performance of inducer B in hydrogen at 30 000 rpm. Net positive suction head, greater than 500 feet (> 152.4 m).

Cavitating performance. - The cavitating performance of inducer B is shown in figure 6 where head-rise coefficient ψ is plotted as a function of inducer net positive suction head NPSH. Several flow coefficients are presented for each of the nominal hydrogen temperatures. The rotative speed is 30 000 rpm for all data. The solid portion of the curves represents the performance with no vapor present at the inducer inlet. The

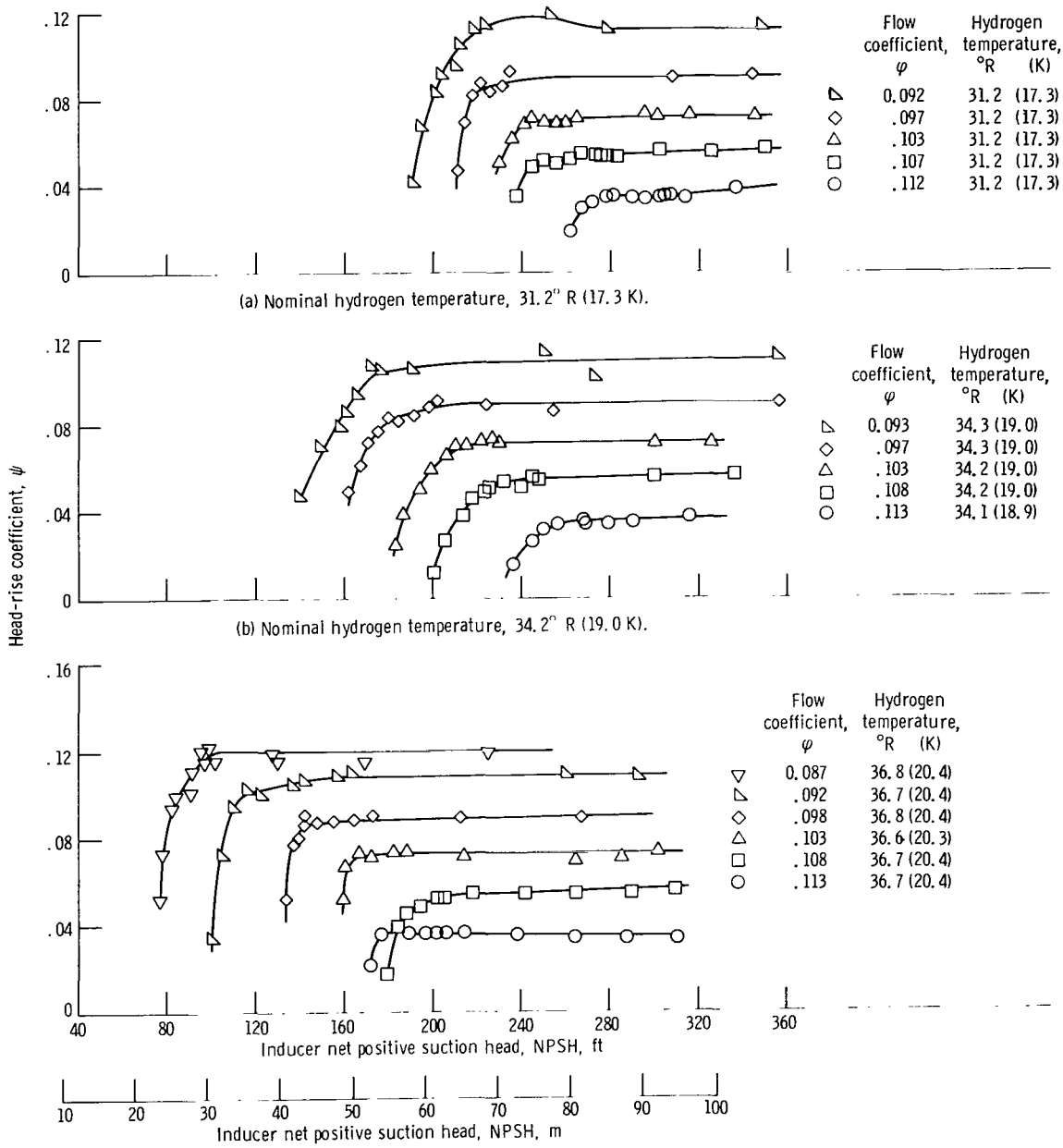

(c) Nominal hydrogen temperature, 36.7° R (20.4 K).

Figure 6. - Cavitation performance of inducer B in hydrogen at 30 000 rpm.

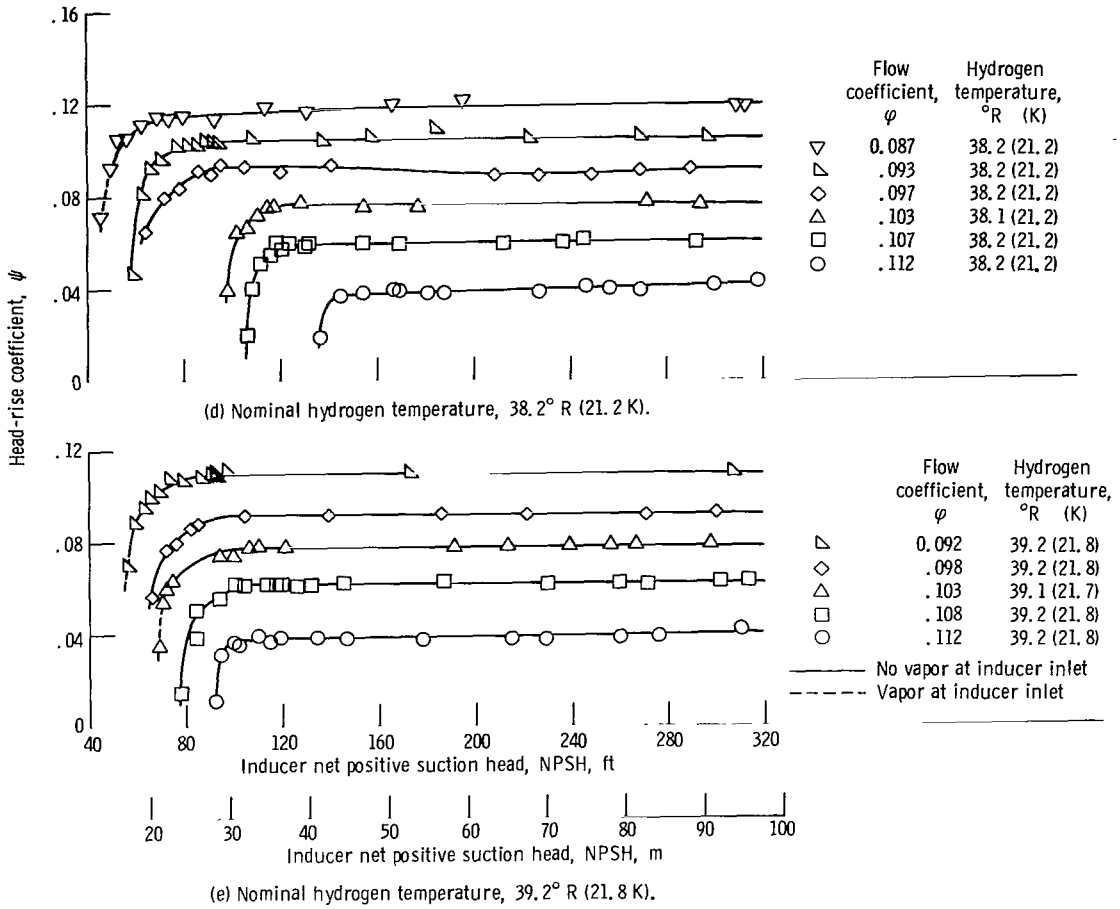

(e) Nominal hydrogen temperature, 39.2° R (21.8 K).

Figure 6. - Concluded.

dashed portion of some of the curves represents the performance with vapor present at the inducer inlet. Vapor was assumed to occur at the inducer inlet when NPSH was less than the inlet fluid velocity head.

In figure 7, the required NPSH for a cavitating-to-noncavitating head-rise-coefficient ratio ψ/ψ_{NC} of 0.70 is plotted as a function of flow coefficient φ. Several nominal hydrogen temperatures are shown for a rotative speed of 30 000 rpm. At a constant flow coefficient, the required NPSH decreased with increasing liquid temperature until the NPSH was essentially equal to the inlet fluid velocity head. Then, no further decrease in NPSH was observed as liquid temperature increased. At a constant liquid temperature, the required NPSH increased with increasing flow coefficient.

The decrease in required NPSH with increasing liquid temperature is attributed to the thermodynamic effects of cavitation.

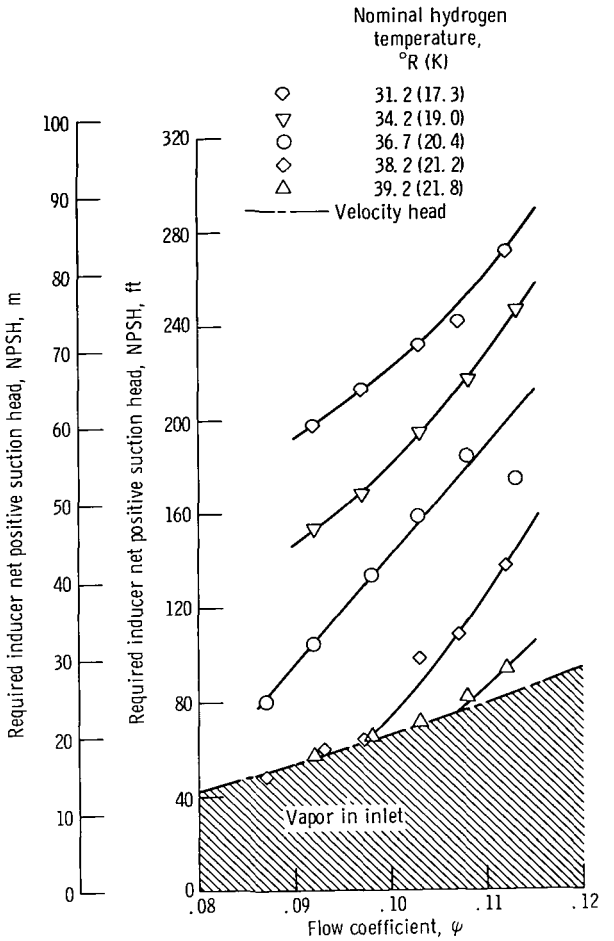

Figure 7. - Variation of inducer B cavitation performance with flow coefficient for several hydrogen temperatures. Rotative speed, 30 000 rpm; head-rise-coefficient ratio, 0.70.

Thermodynamic effects of cavitation. - A method for predicting the thermodynamic effects of cavitation and the cavitation performance of inducers is presented in detail in reference 3. A brief resume of the prediction method is also presented herein. In reference 3, a heat balance between the heat required for vaporization and the heat drawn from the liquid adjacent to the cavity is used to show that the cavity pressure depression (below free-stream vapor pressure) is

$$\Delta h_v = \left(\frac{\rho_v}{\rho_l}\right)\left(\frac{L}{C_l}\right)\left(\frac{dh_v}{dT}\right)\left(\frac{\mathcal{V}_v}{\mathcal{V}_l}\right) \tag{1}$$

With the properties of hydrogen known, values of vapor- to liquid-volume ratio $\mathcal{V}_v/\mathcal{V}_l$ as a function of Δh_v can be obtained by numerical integration of equation (1). This

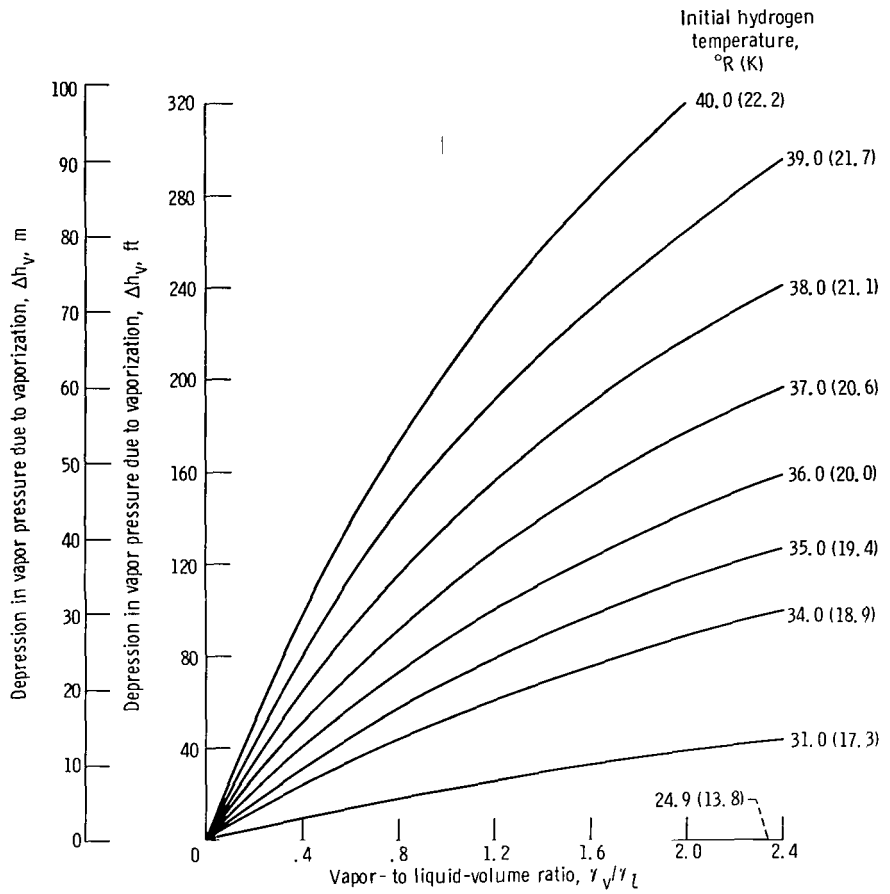

Figure 8. - Calculated vapor pressure depression due to vaporization as function of volume ratio for several liquid hydrogen temperatures.

takes into account changes in properties as the equilibrium temperature drops because of the evaporative cooling. The calculated depression in vapor pressure Δh_v is plotted as a function of vapor- to liquid-volume ratio ψ_v/ψ_l for a range of liquid hydrogen temperatures in figure 8. Equation (1) cannot be used directly to predict the required NPSH because the absolute value of ψ_v/ψ_l is not known. However, it was shown that, if a reference value of ψ_v/ψ_l is established experimentally by determining Δh_v at a given set of operating conditions, values of ψ_v/ψ_l relative to this reference value can be estimated from the following equation:

$$\frac{\psi_v}{\psi_l} = \left(\frac{\psi_v}{\psi_l}\right)_{ref} \left(\frac{\alpha_{ref}}{\alpha}\right)\left(\frac{N}{N_{ref}}\right)^{0.8} \tag{2}$$

This equation assumes geometrically similar cavitating flow conditions (i.e., the same flow coefficient and the same head-rise-coefficient ratio for the predicted condition as those for the reference condition).

The equation for predicting the inducer cavitation performance for a constant flow coefficient and head-rise-coefficient ratio is repeated (from ref. 3) for convenience:

$$\frac{NPSH + \Delta h_v}{NPSH_{ref} + \left(\Delta h_v\right)_{ref}} = \left(\frac{N}{N_{ref}}\right)^2 \tag{3}$$

This relation requires that values of NPSH and N for two experimental test points be available for the inducer of interest. These experimental data can be for any combination of liquid, liquid temperature, or rotative speed, provided that at least one set of data exhibits a measurable thermodynamic effect. From these experimental data, the cavitation performance for the inducer can be predicted for any liquid, liquid temperature, or rotative speed.

The required NPSH for nominal temperatures of 31.2° and 34.2° R (17.3 and 19.0 K) from figure 7 were used as the two experimental curves to calculate the thermodynamic effects of cavitation. The predicted magnitude of the thermodynamic effects of cavitation for inducer B is shown in figure 9 as a function of flow coefficient for several hydrogen temperatures. An iterative solution of equations (1), (2), and (3) is required

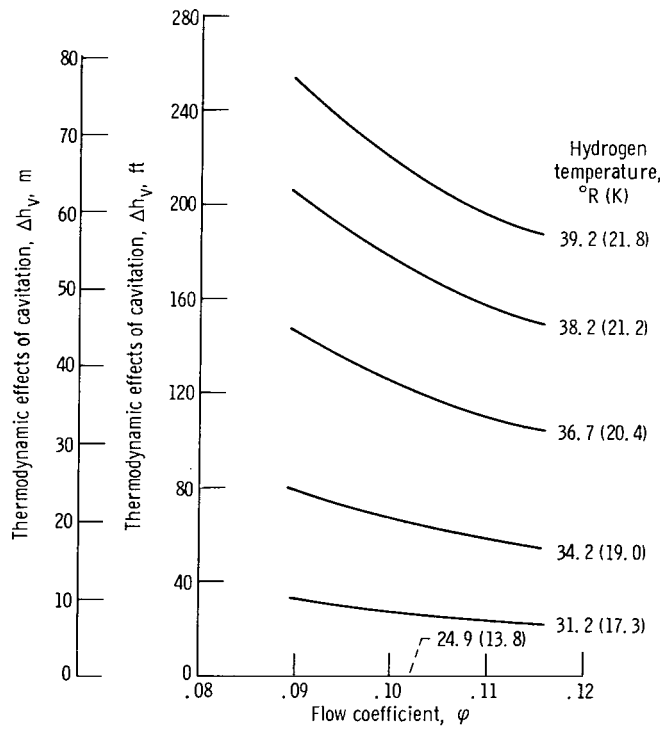

Figure 9. - Predicted thermodynamic effects of cavitation as function of flow coefficient for several hydrogen temperatures for inducer B. Rotative speed, 30 000 rpm; head-rise-coefficient ratio, 0.70.

to determine the reference value of Δh_v. Values of Δh_v at other temperatures were then predicted using equation (1) and the volume ratio obtained from equation (2). The predicted thermodynamic effects of cavitation (fig. 9) increase with increasing liquid temperature and decrease with increasing flow coefficient.

A comparison between experimental and predicted values of required NPSH for inducer B is shown in figure 10. The data points are repeated from figure 7, as are the reference data (solid lines) at 31.2° and 34.2° R (17.3 and 19.0 K) that were used to predict the required NPSH at the other temperatures. The experimental hydrogen data

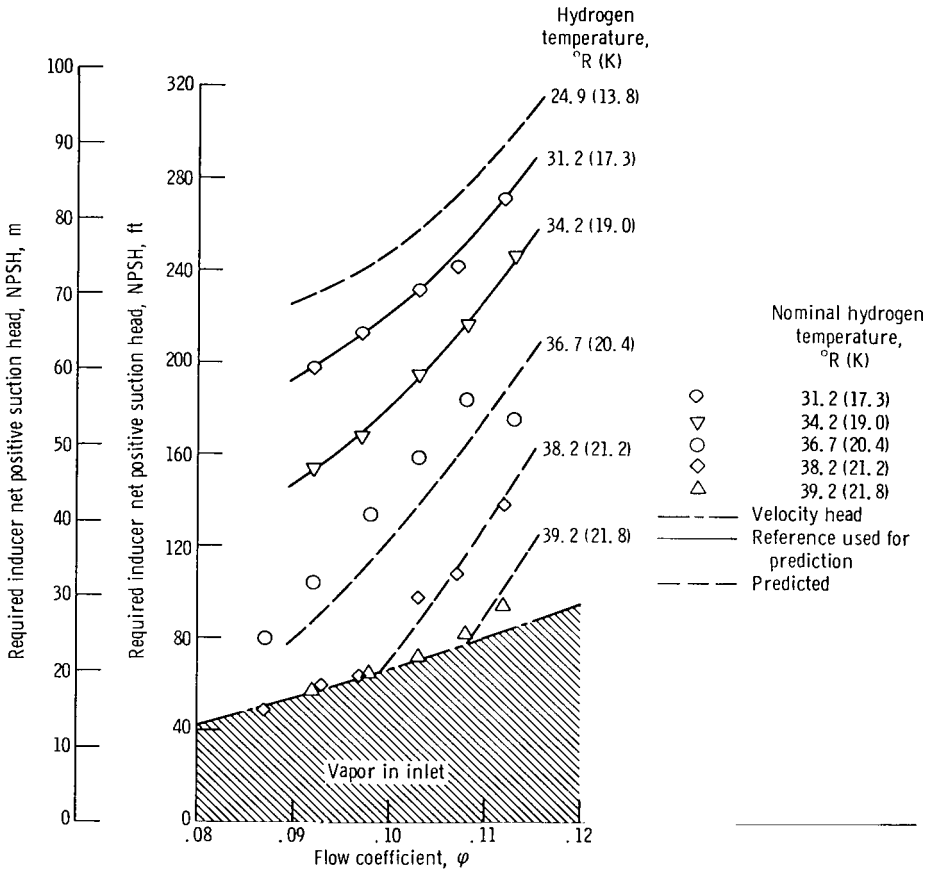

Figure 10. - Comparison of predicted and measured net positive suction head for inducer B in hydrogen. Rotative speed, 30 000 rpm; head-rise-coefficient ratio, 0.70.

compare reasonably well with the predicted curves at values of NPSH above the inlet line vapor region. Values of NPSH less than the calculated velocity head are indicated by the shaded area.

Effect of Blade Leading Edge Thickness

Noncavitating performance. - The effect of blade leading edge thickness on the noncavitating performance is shown in figure 11. The head-rise coefficient ψ is plotted as a function of flow coefficient φ for each of the three inducers. Inducer A, with the thinnest blade leading edge, has the highest head-rise coefficient over the entire flow range. Inducer C, with the thickest blade leading edge, has the lowest head-rise coefficient. This is attributed to the greater leading edge blockage associated with a thicker leading edge.

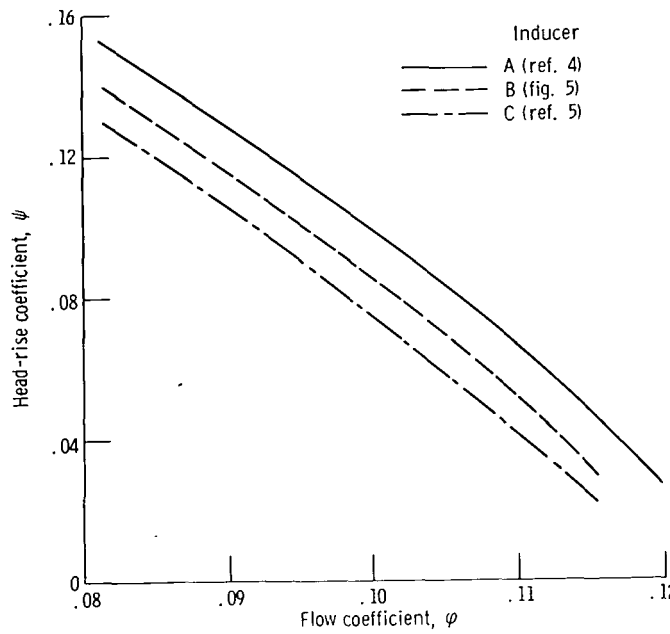

Figure 11. - Effect of blade leading edge thickness on noncavitating performance of 80.6 helical inducer in hydrogen.

Cavitating performance. - The effect of blade leading edge thickness on the cavitating performance is shown in figure 12. The required net positive suction head NPSH for a head-rise-coefficient ratio ψ/ψ_{NC} of 0.70 is plotted as a function of flow coefficient. Several liquid temperatures are shown for each inducer operated at a rotative speed of 30 000 rpm. The effect of blade leading edge thickness on the cavitation performance varies with flow coefficient and liquid temperature. At a nominal liquid temperature of 36.6° R (20.3 K), the required NPSH is lowest for inducer A over the entire flow range. However, at a nominal liquid temperature of 31.0° R (17.2 K), the required NPSH is lowest for inducer A at the lowest flow coefficients and is lowest for inducer B at the highest flow coefficients.

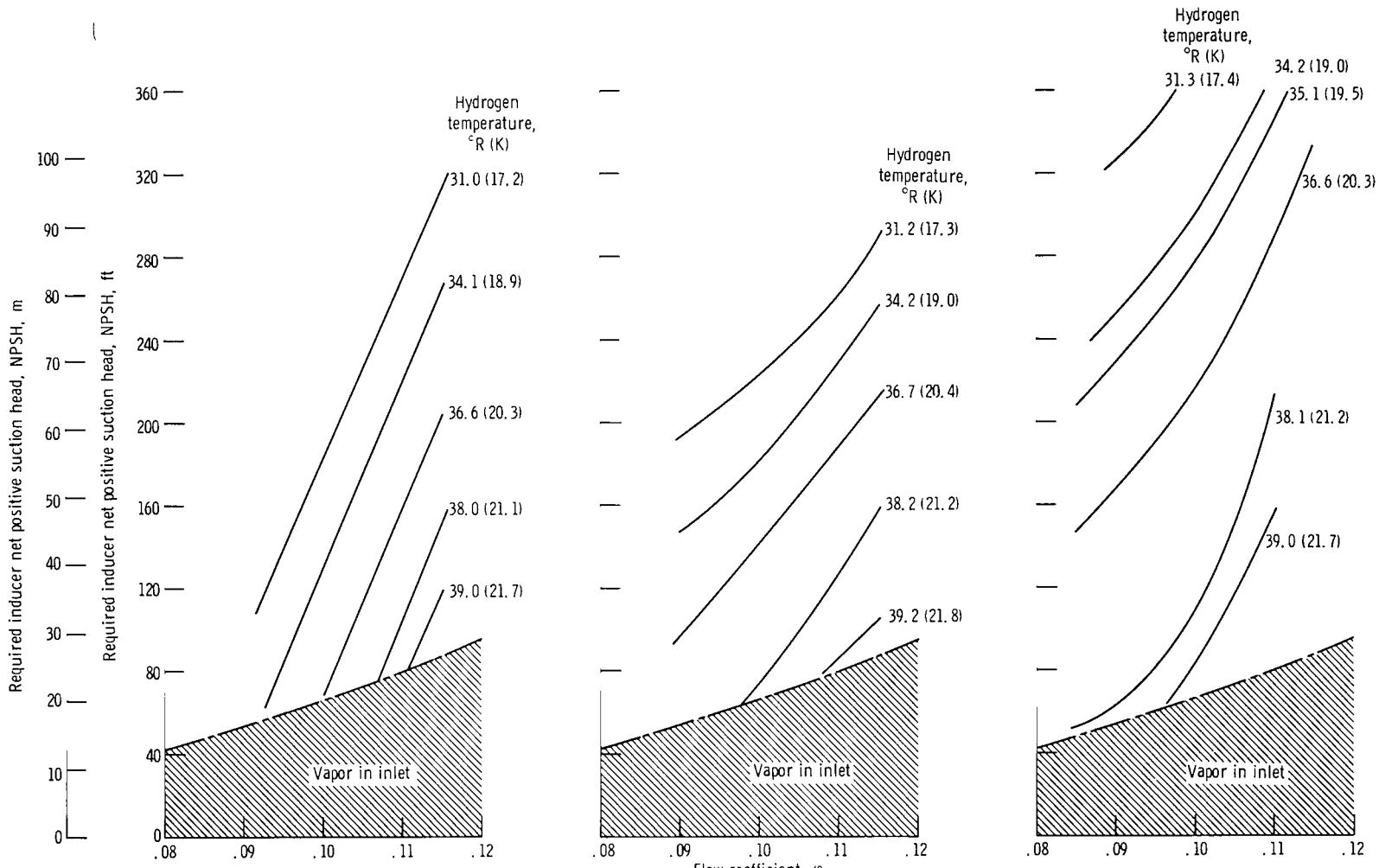

(a) Inducer A (ref. 4).

(b) Inducer B (fig. 7).

(c) Inducer C (ref. 5).

Figure 12. - Effect of blade leading edge thickness on cavitation performance of 80.6° helical inducer in hydrogen. Rotative speed, 30 000 rpm; head-rise-coefficient ratio, 0.70.

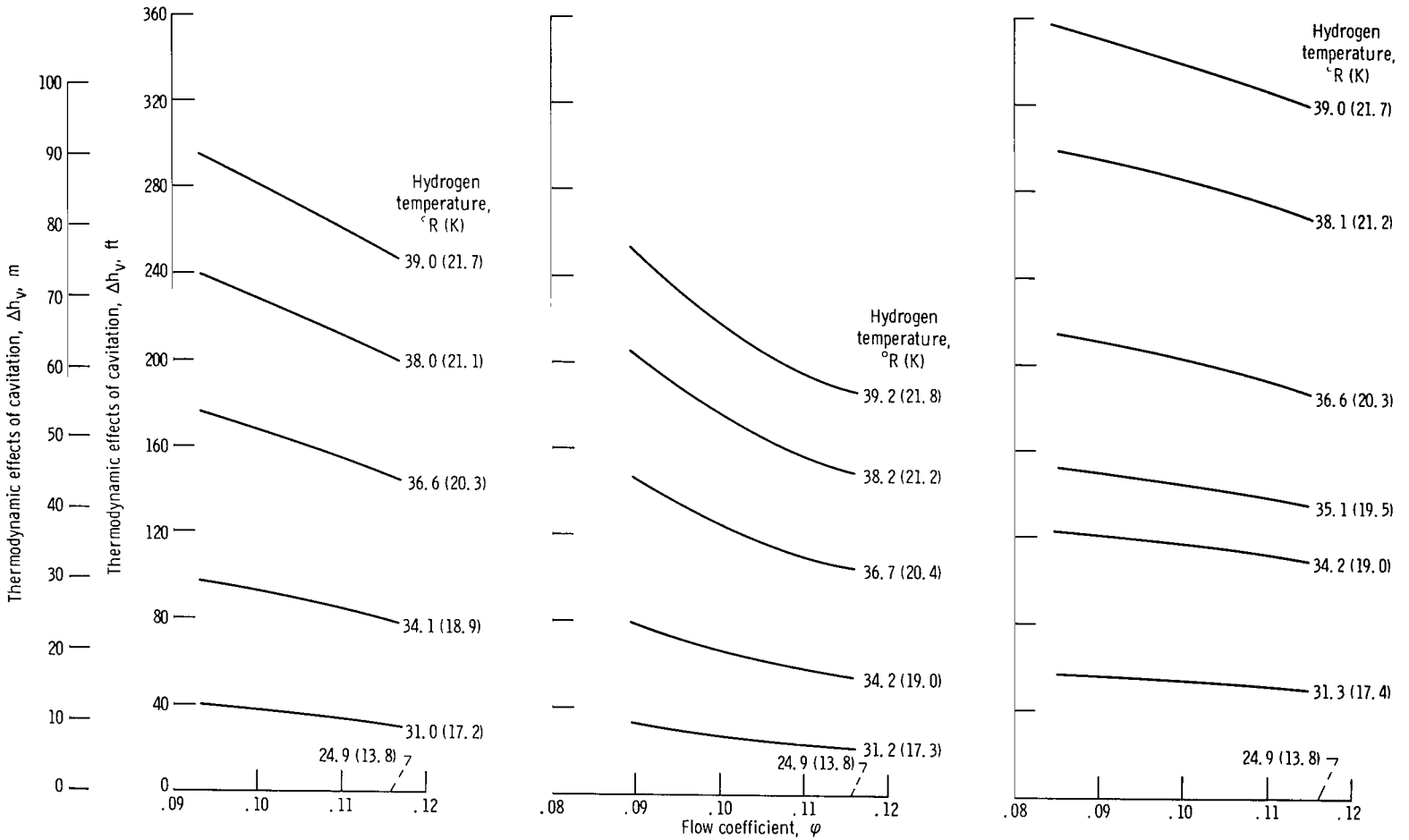

(a) Inducer A (ref. 4).

(b) Inducer B (fig. 9).

(c) Inducer C (ref. 5).

Figure 13. - Effect of blade leading edge thickness on predicted thermodynamic effects of cavitation for 80.6° helical inducer in hydrogen. Rotative speed, 30 000 rpm; head-rise-coefficient-ratio, 0.70.

Thermodynamic effects of cavitation. - The variation in the thermodynamic effects of cavitation with blade leading edge thickness is shown in figure 13. The predicted Δh_v values are for a rotative speed of 30 000 rpm and a head-rise-coefficient ratio of 0.70. For all three inducers, the thermodynamic effects increase with increasing liquid temperature and decrease with increasing flow coefficient. For a constant liquid temperature and flow coefficient, the thermodynamic effects of cavitation are the smallest for inducer B and the greatest for inducer C.

Cavitation Parameters

As shown herein and in references 2 to 5, the cavitation performance, as measured by both the required NPSH and the magnitude of the thermodynamic effects of cavitation, varies with the liquid, liquid temperature, rotative speed, flow coefficient, and inducer design. Thus, when values of NPSH and Δh_v are quoted, they must be accompanied by each of the variables. Therefore, two cavitation parameters that qualitatively evaluate the cavitation performance will be developed.

A more convenient way to express the cavitation performance is to rewrite equation (3) in the following manner:

$$\text{K-factor} = \frac{\text{NPSH} + \Delta h_v}{\frac{V^2}{2g}} = \frac{\text{NPSH}_{ref} + \left(\Delta h_v\right)_{ref}}{\frac{V_{ref}^2}{2g}} \tag{4}$$

The inlet axial velocity V has been used instead of the rotative speed N to make the equation dimensionless. The velocity V is proportional to N, thereby allowing this substitution. With the K-factor known, the cavitation performance of an inducer operated in a liquid without thermodynamic effects can be evaluated. The greater K-factor will result in the greater required NPSH.

Another way to evaluate the thermodynamic effects of cavitation is to express the reference values in equation (2) as

$$\text{M-factor} = \left(\frac{\gamma_v}{\gamma_l}\right)_{ref} \alpha_{ref}\left(\frac{1}{V_{ref}}\right)^{0.8} \tag{5}$$

With the substitution of equation (5), equation (2) becomes

$$\left(\frac{\gamma_v}{\gamma_l}\right) = \text{M-factor}\left(\frac{1}{\alpha}\right)(V)^{0.8} \tag{6}$$

Equation (6) can then be used in conjunction with equation (1) or the curves of figure 8 to determine the Δh_v values for the conditions of interest. Thus, only the M-factor has to be known to qualitatively evaluate the inducer that will have the greatest thermodynamic effects of cavitation. For a given temperature and rotative speed, the inducer with the greater M-factor will have the greater thermodynamic effects.

The cavitation parameters, M-factor and K-factor, are plotted in figure 14 as a function of flow coefficient for the three inducers. M-factor shows the same trend with inducer as did the thermodynamic effects of cavitation. M-factor is the smallest for inducer B and the greatest for inducer C. For all three inducers, M-factor decreased with increasing flow coefficient.

As can be observed from figure 14(b), the K-factor is a more convenient parameter for comparing the cavitation performance of the three inducers than were the curves of figure 12. The K-factor did not show a consistent trend with blade leading edge thickness. The K-factor for inducer C (thickest blade leading edge) was greatest over the entire flow range. At a flow coefficient of less than 0.106, the K-factor was the smallest for inducer A (thinnest blade leading edge), whereas at a flow coefficient greater than 0.106, the K-factor was the smallest for inducer B. For inducers B and C, the K-factor

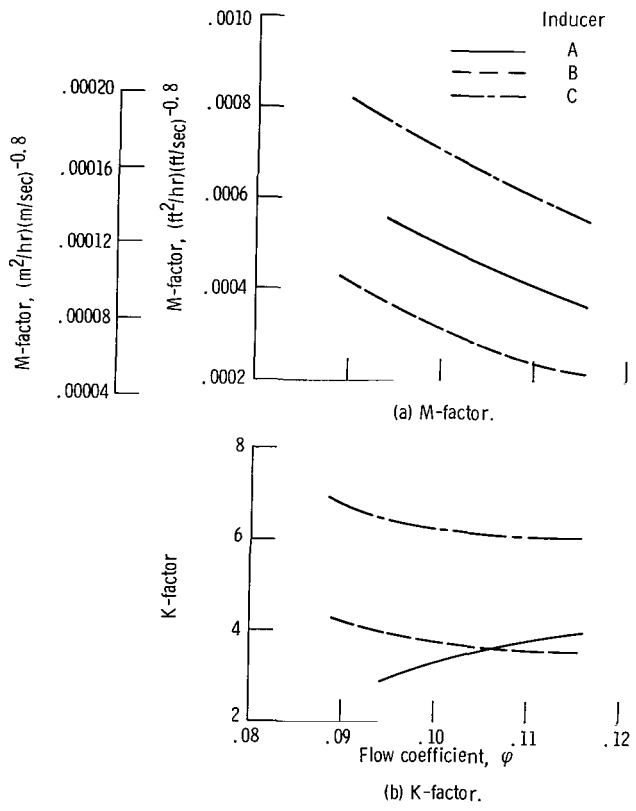

Figure 14. - Effect of blade leading edge thickness on cavitation parameters for 80.6° helical inducer in hydrogen. Head-rise-coefficient ratio, 0.70.

decreased with increasing flow coefficient. However, for inducer A, the K-factor increased with increasing flow coefficient.

The values of Δh_v and NPSH can be obtained from the cavitation parameters, M-factor (eq. (5)) and K-factor (eq. (4)). For example, the M-factor for inducer B will yield the Δh_v values shown on the curves of figure 9. The K-factor for inducer B can be used to calculate the required NPSH values shown in figure 10 for liquid hydrogen at 24.9° R (13.8 K). The values of Δh_v obtained from the M-factor are then subtracted from the required NPSH at 24.9° R (13.8 K) to obtain the required NPSH at other liquid temperatures (fig. 10).

SUMMARY OF RESULTS

Three different 80.6° helical inducers were tested in liquid hydrogen at a rotative speed of 30 000 rpm. These inducers were identical in design except for the blade leading edge thickness. The experimental inducers were tested over a liquid temperature range of 31.0° to 39.2° R (17.2 to 21.8 K) for flow coefficients from 0.082 to 0.118. The net positive suction head NPSH requirements were measured for each inducer. The measured required NPSH was used in conjunction with a semiempirical prediction method to predict the magnitude of the thermodynamic effects of cavitation. This investigation yielded the following principal results:

1. The required NPSH for a head-rise-coefficient ratio of 0.70 was considerably different for the three blade leading edge thicknesses. Although no consistent trend with thickness was observed, the required NPSH for the inducer with the thickest blade leading edge was generally greater than that for the other two inducers. The required NPSH for each thickness increased with increasing flow coefficient and decreased with increasing liquid temperature.

2. The inducer with the thickest blade leading edge exhibited the greatest thermodynamic effects of cavitation. The inducer with a medium-thin blade leading edge showed the smallest thermodynamic effects of cavitation.

3. Two cavitation parameters were developed that qualitatively evaluate the cavitation performance of inducers. The parameter K-factor evaluates the pressure requirements, and the parameter M-factor evaluates the thermodynamic effects of cavitation.

4. The inducer that had the thinnest blade leading edge had the highest noncavitating head rise over the entire flow range. The inducer that had the thickest blade leading edge had the lowest noncavitating head rise.

Lewis Research Center,
National Aeronautics and Space Administration,
Cleveland, Ohio, April 6, 1970,
128-31.

APPENDIX - SYMBOLS

C_l	specific heat of liquid, Btu/(lbm)(^{o}R); J/(kg)(K)
dh_v/dT	slope of curve of vapor pressure head against temperature, ft/^{o}R; m/K
g	acceleration due to gravity, ft/sec^2; m/sec^2
ΔH	pump head rise based on inlet density, ft of liquid; m of liquid
Δh_v	decrease in vapor pressure because of vaporization (magnitude of thermodynamic effect of cavitation), ft of liquid; m of liquid
k	liquid thermal conductivity, Btu/(hr)(ft)(^{o}R); J/(hr)(m)(K)
L	latent heat of vaporization, Btu/lbm; J/kg
N	rotative speed, rpm
NPSH	net positive suction head, ft of liquid; m of liquid
U_t	blade tip speed, ft/sec; m/sec
V	average axial velocity at inducer inlet, ft/sec; m/sec
$\mathcal{V}_l$	volume of liquid involved in cavitation process, in.^{3}; cm^3
$\mathcal{V}_v$	volume of vapor, in.^{3}; cm^3
α	thermal diffusivity of liquid, $k/\rho_l C_l$, ft^2/hr; m^2/hr
ρ_l	density of liquid, lbm/ft^3; kg/m^3
ρ_v	density of vapor, lbm/ft^3; kg/m^3
φ	flow coefficient, V/U_t
ψ	head-rise coefficient, $g\,\Delta H/U_t^2$
ψ/ψ_{NC}	cavitating-to-noncavitating head-rise-coefficient ratio

Subscripts:

NC	noncavitating
ref	reference value obtained from experimental tests

REFERENCES

1. Ball, Calvin L.; Meng, Phillip R.; and Reid, Lonnie: Cavitation Performance of 84° Helical Pump Inducer Operated in 37° and 42° R Liquid Hydrogen. NASA TM X-1360, 1967.

2. Meng, Phillip R.: Change in Inducer Net Positive Suction Head Requirement with Flow Coefficient in Low Temperature Hydrogen (27.9° to 36.6° R). NASA TN D-4423, 1968.

3. Ruggeri, Robert S.; and Moore, Royce D.: Method of Prediction of Pump Cavitation Performance for Various Liquids, Liquid Temperatures, and Rotative Speeds. NASA TN D-5292, 1969.

4. Moore, Royce D.; and Meng, Phillip R.: Thermodynamic Effects of Cavitation of an 80.6° Helical Inducer Operated in Hydrogen. NASA TN D-5614, 1970.

5. Meng, Phillip R.; and Moore, Royce D.: Hydrogen Cavitation Performance of 80.6° Helical Inducer with Blunt Leading Edges. NASA TM X-2022, 1970.

6. Moore, Royce D.; Ruggeri, Robert S.; and Gelder, Thomas F.: Effects of Wall Pressure Distribution and Liquid Temperature on Incipient Cavitation of Freon-114 and Water in Venturi Flow. NASA TN D-4340, 1968.

7. Meng, Phillip R.; and Moore, Royce D.: Hydrogen Cavitation Performance of 80.6° Helical Inducer Mounted in Line with Stationary Centerbody. NASA TM X-1935, 1970.

NASA-Langley, 1970 —— 12 E-5445

NATIONAL AERONAUTICS AND SPACE ADMINISTRATION
WASHINGTON, D. C. 20546

OFFICIAL BUSINESS

FIRST CLASS MAIL

POSTAGE AND FEES PAID
NATIONAL AERONAUTICS A
SPACE ADMINISTRATION

060 001 37 51 3DS 70151 00903
AIR FORCE WEAPONS LABORATORY /WLOL/
KIRTLAND AFB, NEW MEXICO 87117

ATT E. LOU BOWMAN, CHIEF,TECH. LIBRARY

eliverable (Section 15
Postal Manual) Do Not Retu

"The aeronautical and space activities of the United States shall be conducted so as to contribute . . . to the expansion of human knowledge of phenomena in the atmosphere and space. The Administration shall provide for the widest practicable and appropriate dissemination of information concerning its activities and the results thereof."

—NATIONAL AERONAUTICS AND SPACE ACT OF 1958

NASA SCIENTIFIC AND TECHNICAL PUBLICATIONS

TECHNICAL REPORTS: Scientific and technical information considered important, complete, and a lasting contribution to existing knowledge.

TECHNICAL NOTES: Information less broad in scope but nevertheless of importance as a contribution to existing knowledge.

TECHNICAL MEMORANDUMS: Information receiving limited distribution because of preliminary data, security classification, or other reasons.

CONTRACTOR REPORTS: Scientific and technical information generated under a NASA contract or grant and considered an important contribution to existing knowledge.

TECHNICAL TRANSLATIONS: Information published in a foreign language considered to merit NASA distribution in English.

SPECIAL PUBLICATIONS: Information derived from or of value to NASA activities. Publications include conference proceedings, monographs, data compilations, handbooks, sourcebooks, and special bibliographies.

TECHNOLOGY UTILIZATION PUBLICATIONS: Information on technology used by NASA that may be of particular interest in commercial and other non-aerospace applications. Publications include Tech Briefs, Technology Utilization Reports and Notes, and Technology Surveys.

Details on the availability of these publications may be obtained from:

SCIENTIFIC AND TECHNICAL INFORMATION DIVISION

NATIONAL AERONAUTICS AND SPACE ADMINISTRATION

Washington, D.C. 20546